BRUSH TIRE MODEL WITH INCREASED FLEXIBILITY

Jacob Svendenius[*], **Björn Wittenmark**[†]

[*] Haldex Brake Products AB
Box 501, SE-261 24 Landskrona, Sweden,
phone: +46 418 47 62 40, fax: +46 418 47 60 01,
email:jacob.svendenius@haldex.com

[†] Department of Automatic Control, Lund Institute of Technology,
Box 118, SE-221 00 Lund, Sweden,
phone: +46 46 222 87 88, fax: +46 46 13 81 18,
email:bjorn@control.lth.se

Keywords: Friction estimation, Brush tire model, Tire-road friction, Longitudinal slip, Pressure distribution

Abstract

This article covers a method to make the description of the force-slip curve generated by the brush tire model more flexible. A calibration factor is applied to make the slope more or less convex. The main use is in car applications where road friction estimation is a major issue. If the real tire characteristic differs from the model there will be a bias in the estimation and a higher brake force is needed before a reliable friction coefficient can be estimated. Introduction of calibration parameters is a way to enhance the estimation, specially at lower brake forces.

1 Introduction

There are several ways to describe the relation between the generated force and the slip of a car tire. The most widely used is the Magic Formula, an empirical tire model including five parameters, see Section 2.2. To obtain good values of the parameters, measurements from the whole slip range $\kappa_x \in [0,1]$ are necessary. If only low slip values are available the Magic Formula is too flexible and an extrapolation to values outside the measurement region is not always possible. The brush tire model is not that flexible and it includes only two parameters. The advantage is then that only by regarding low slip values, estimation of the curve at higher slip is possible. A drawback is that the mismatch to the real data can be larger since approximations have been done in the modeling. The stiffness in the model also makes it hard to adjust for unmodeled effects. This article covers a method to make the description of the force-slip curve generated by the brush tire model more flexible. A calibration factor is introduced to make the slope more or less convex. For the further reading it is necessary to clearify the definition of the slip, since it can be defined in several ways. The difference between the general definitions is the normalization of the slip velocity. The notation is shown in Table 1, where the velocity vector of the wheel, $\overline{v}$, has the components, v_x and v_y. The slip velocity is denoted $v_{sx} = v_x - \Omega R_d$, where Ω is the rotational speed of the wheel and R_d the dynamical radius. The index x denotes the longitudinal and y the lateral direction.

Origin	Notation	Long.	Lateral
SAE, ISO	κ	v_{sx}/v_x	v_y/v_x
SAE praxis	s	$v_{sx}/\overline{v}$	$v_y/\overline{v}$
Physical	σ	$v_{sx}/(\Omega R_d)$	$v_y/(\Omega R_d)$

Table 1: Slip definitions.

For the braking case the SAE praxis is the most convenient definition, since it the always stays between -1 and 1. The other definitions get singular either at wheel lock or at zero lateral speed. For the driving case σ is most often used. In Section 2 we derive an expression for the force, depending on σ_x, which corresponds to the deformation in the tire. Hence, it is a physically motivated definition. For the empirical modeling the main thing is not how to define the slip, but rather to know which definition that has been used for the measurements.

2 Review of the brush tire model

The brush model, see [4], relies on the assumption that the slip is caused by deformation of the rubber material between the tire carcass and the ground. The material is approximated as small brush elements attached to the carcass, which is assumed to be stiff, see Figure 1. The carcass can still flex toward the hub, but it can neither stretch nor shrink. Every brush element can deform independently of the other.

2.1 Longitudinal force-slip model

A brush element i comes in contact with the road at time t=0 and position $x = a$. The position can be defined either by the bristles upper point (x_{ic}, attached to the carcass) or by its lower point (x_{ir}, the contact to the road), which is illustrated by Figure 2. As long as there is no sliding the positions are:

$$x_{ci} = a - \int_0^t \Omega R_d \, dt \tag{1}$$

$$x_{ri} = a - \int_0^t v_x \, dt \tag{2}$$

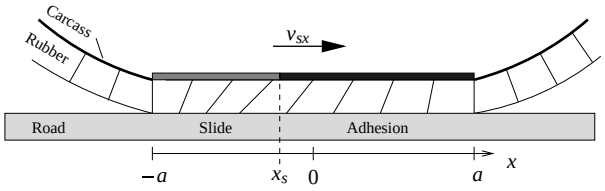

Figure 1: Illustration showing the deformation of the rubber layer between the tire carcass and the road according to the brush model. The carcass moves with the velocity v_{sx} relative the road. The contact zone moves with the vehicle velocity v_x.

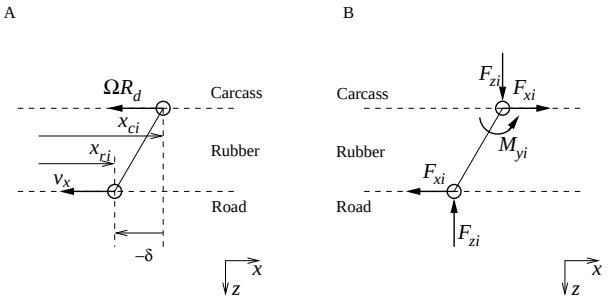

Figure 2: The relative velocity and the position of upper and lower point of a brush element is shown in A. Figure B shows the force equilibrium of the element. The additional torque M_{yi} working on the element to get rotational balance is not used in any calculations.

The deformation of the element is:

$$\delta_i = x_{ci} - x_{ri} = \int_0^t v_x - \Omega R_d \, dt = \int_0^t v_{sx} \, dt \tag{3}$$

If constant velocities are assumed, (3) together with (1) or (2) gives

$$\delta_i = \frac{v_{sx}}{\Omega R_d}(a - x_{ci}) = \frac{v_{sx}}{v_x}(a - x_{ri}) \tag{4}$$

where $v_{sx}/\Omega R_d$ is the longitudinal slip denoted σ_x.

Rubber does not necessarily deform linearly, but it is approximated in that way. The force needed to achieve the amount of deformation given in (3) is then

$$F_{xi} = k\delta_i \tag{5}$$

The deformation of a bristle is limited by the friction between the tire and the road and the maximum force acting on the brush element is given by

$$F_{xi,max} = \mu F_{zi} \tag{6}$$

Putting (5) and (6) together the maximal deformation can be expressed as

$$\delta_{i,max} = \frac{\mu F_{zi}}{k} \tag{7}$$

The brush element starts to slide when the deformation reaches this value. The force acting on the bristle is then μF_{zi}. Three different choices for the entire contact patch arises.

- Adhesion in the entire contact area. The slip curve is only depending on the rubber properties.
- Both sliding and adhesion. The contact area is split into two sections, one with adhesion and one with sliding.
- The entire tire surface slides against the ground. The braking force is then only depending on the friction coefficient at the actual condition.

When both adhesion and sliding occurs in the contact patch it is possible to calculate the position where the sliding starts, the so called breakaway point. Use of (4) and (7) renders

$$x_{cis} = a - \frac{\mu F_{zi} \Omega R_d}{v_{sx} k} \tag{8}$$

The partition of the contact patch into discrete bristle elements is abandoned and an integration over the whole contact length is performed instead. The following changes, $k = c_p \, dx_c$ and $F_{zi} = q_z(x_c) \, dx_c$ are introduced, where c_p denotes stiffness per length unit and q_z is the vertical force per length unit between tire and road. Adding the force from the area of adhesion to the force from the sliding region the total braking force is

$$F_x = \int_{x_{cs}}^{a} c_p \frac{v_{sx}}{\Omega R_d}(a - x_c) dx_c + \int_{a}^{x_{cs}} q_z(x_c) \mu dx_c \tag{9}$$

It can be discussed whether to use x_r or x_c in the the formulas. For the vertical force $F_{zi} = q_z(x_{ci})$, x_r might be used instead of x_c, while the pressure distribution usually is defined between the tire and the road. However, since the bristles are attached to the carcass they are equally spaced there, i.e. dx_c is constant. dx_r is not constant along the contact length and then not suitable as integration variable. From now on the index c is dropped and x denotes the carcass position of the bristle. The vertical pressure distribution is assumed to be parabolic,

$$q_z(x) = \frac{3F_z}{4a}\left(1 - \left(\frac{x}{a}\right)^2\right) \tag{10}$$

and the situation is as illustrated in Figure 3. Curve no. 1 is the maximum available friction force $\mu q_z(x)$ according to the pressure distribution. Line 2 is the theoretical force needed to deform the bristles due to the velocity difference v_{sx} according to (4) together with (5). The incline of this line is $-c_p \sigma_x$. The marked area is the total force from the resulting brush deformation. The first contact choice with only adhesion can not be achieved assuming this pressure distribution, since sliding will occur somewhere in the region as long as the slip is nonzero. The breakaway point x_s can be derived from the following formula:

$$c_p \sigma (a - x_s) = \mu q_z(x_s) \tag{11}$$

Evaluating (9) with the pressure distribution given by (10) the equation for the force-slip will be

$$F_x = 2c_p a^2 \sigma_x - \frac{4}{3}\frac{(c_p a^2 \sigma_x)^2}{\mu F_z} + \frac{8}{27}\frac{(c_p a^2 \sigma_x)^3}{(\mu F_z)^2} \tag{12}$$

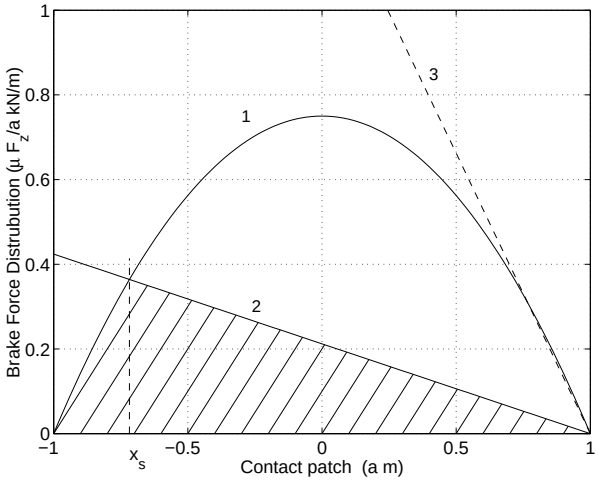

Figure 3: Picture showing the deformation of the rubber layer between carcass and road. Curve 1: Maximum available friction force per length unit (l.u.) μq_z. Curve 2: Force per l.u. necessary for the deformation of the rubber bristles due to the velocity difference. Curve 3: Corresponds to the slip where there are no adhesion in the contact patch (σ_x°).

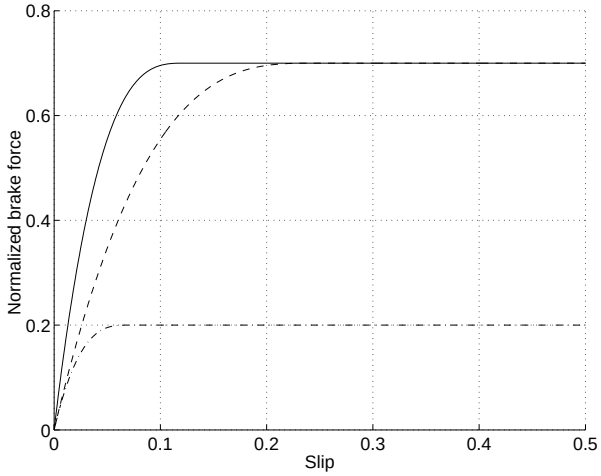

Figure 4: Normalized brake force contra longitudinal slip (σ_x) using the brush tire model with different values of μ and c_p.

According to this expression the slip behavior is mainly dependent on the tire properties at low slip. Often the relation between the force and the slip in this region is assumed to be linear with a coefficient called braking stiffness C_x. In this case $C_x = 2c_p a^2$. At higher slip the friction coefficient is the major source for the characteristics. If the inclination of line 2 in Figure 3 is steeper than the inclination of curve 1 at $x = a$ the entire surface will slide, which is illustrated by line 3. Hence, the incline of the pressure distribution at $x = a$ sets the slip limit where the entire rubber surface starts to slide against the road. In this case it is given by

$$\sigma_x^\circ = \frac{3}{2}\frac{\mu F_z}{c_p a^2} \tag{13}$$

For slip exceeding this value the braking force will simply be $F_x = \mu F_z$. The resulting force-slip function is plotted in Figure 4. Since constant friction is assumed, the brake force is constant for slip values above σ_x°.

2.1.1 Discussion

This section has mainly treated the way to physically derive a relation between the braking force and the slip. The formula includes the rubber stiffness c_p, the length of the contact patch $2a$, the tire/road friction μ, and the vertical wheel load F_z. The vertical pressure distribution $q_z(x)$ is another very important factor for the formula. c_p is a material parameter depending on the rubber thickness, temperature, age, etc. The contact length depends on the pressure inside the tire and the wheel load F_z. The friction is the most uncertain parameter and it is affected by certain factors as road condition, slip velocity, and tread thickness.

2.2 Empirical model

There exist several empirical models that describe the input-output formulas for a tire. The most well-known is the Magic Formula, presented by H. B. Pacejka in [1], and is used as reference curve in this paper. It is represented as

$$F_x = D\sin\left(C\arctan\left(B\kappa - E\left(B\kappa - \arctan B\kappa\right)\right)\right) \tag{14}$$

The parameters B, C, D, and E have to be identified from measurement data. Both the longitudinal and lateral force can be expressed in this form. κ denotes the slip in the corresponding direction, see Section 1.

3 Modified brush tire model

The brush tire model presented in Section 2 is widely used to estimate the friction coefficient between the tire and the road, see for instance [3] and [5]. The advantage of the brush model is its simplicity. It only includes two parameters to describe the shape of the force-slip curve, the braking stiffness $2c_p a^2$ and the maximal friction force μF_z. By knowing only these two parameters the slip characteristic up to the brake force peak can be determined. The parameters can be estimated by measurements of the real tire characteristic even at rather low tire slip. As seen in Section 2 some approximations has been done when deriving (12) and the result does not always agree exactly with real tire characteristics. A legitimate question is how such an error affects the parameter prediction. In Figure 5 the brush model is compared to a Magic Formula estimation from a measurement of a real tire. The slip on the x-axis is the SAE standard definition κ_x defined by $(v_x - \Omega R_d)/v_x$ and since the input for the brush model is $\sigma_x = (v_x - \Omega R_d)/\Omega R_d$ it has been rescaled by the relation $\sigma_x = \kappa_x/(1-\kappa_x)$. The curves agree well with each other, but the fact that the measurement has been done on a test bench and the Magic Formula approximation might not exactly cover the true characteristics must be considered.

These circumstances can make the fit of the brush model to the reality both better or worse, probably worse. An estimation of the friction μ at low slip gives a better estimate if the agreement to the real curve is good at slip values where the effect of the second order term, from (12), starts to be noticeable. A way to compensate the behavior of the brush model in this area and make it more flexible could be a useful way to calibrate the μ estimation. In the following, a calibration parameter is introduced to make the brush tire model more flexible, by use of a changable pressure distribution. It could also be done by assuming a velocity dependent friction coefficient, which is further developed in [6].

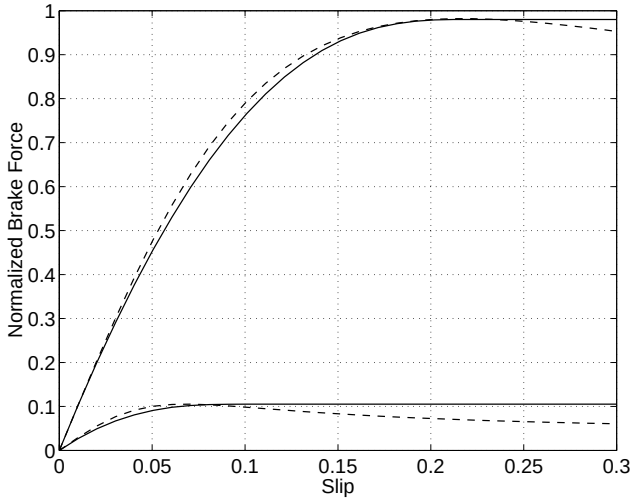

Figure 5: Comparison of brush tire model (solid line) and a Magic Formula realization of real tire data (dashed line) from [2]. The different sets of curves are from road foundations with different friction.

3.1 Pressure distribution

The usual derivation of the brush tire model assumes a parabolic function to describe the vertical pressure distribution between the tire and the road. In this section different distributions are introduced and their effect on the force-slip relation is examined. The new proposal is an asymmetric third order approach with an extra parameter to change its asymmetric properties. The equation is scaled so the total force is equal to F_z. The distribution is only defined in the longitudinal direction and it is supposed to be the average value of the distribution in the lateral direction. The pressure distribution defined by (10) used in Section 2 is now changed to

$$q_z(x) = \frac{3F_z}{4a}\left(1-\left(\frac{x}{a}\right)^2\right)\left(1+d\,\frac{x}{a}\right) \qquad (15)$$

The factor d enables movement of the point of the maximal pressure to the left or to the right. The value on d has to stay in the range of $|d|<1$, otherwise negative pressure values occurs within some parts of the contact patch. Examples of the curve for some values on d are shown in Figure 6. It is difficult to determine the choice of d giving the best coherence to real case. In fact, the pressure distribution, generally variates widely depending on the circumstances. For the static case the vertical pressure may not exceed the tire pressure. If the tire deformation is large enough this value is reached in a region around the center of the contact patch. Since the tire deforms continuously during rolling, the damping and the mass forces due to the deformation increase the pressure at the leading side and decrease it on the trailing side. The center of the vertical force then moves slightly forward for a rolling tire. The third order function with a positive d is a good choice then. The situation also changes when the tire developes a force in the horizontal plane. A brake force would, for instance, make the carcass strained in the leading end and compressed in the trailing end. This would probably increase the movement of the vertical pressure forward and d could reach even a higher value. Usually, the center of the vertical force moves in the opposite direction as the developed tire force is working. A correct choice of pressure distribution needs a lot of further investigation and measurements. Later on the effect of different distributions on the force-slip curve is studied and it is shown that the choice of d might not be done on theoretical foundations.

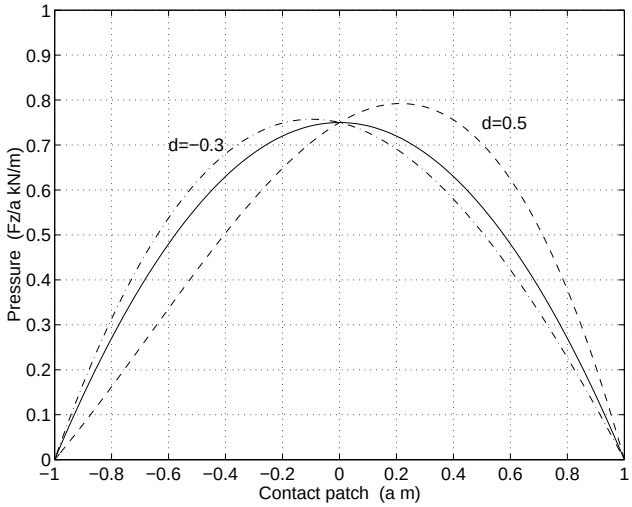

Figure 6: Plot of variants of the proposed pressure distribution. The wheel is supposed to move to the right. The leading side is then to the right and the trailing side is accordingly to the left. The solid line shows the pressure distribution according to equation (10), the dashed and the dashed dotted curve to equation (15) with different choices on d.

3.1.1 Force-slip function

Curve 1 in Figure 3 is now exchanged by (15) and by eliminating the root $x_s = a$ from (11) the breakaway point can be derived by

$$\frac{3Fz\mu}{4a^2}\left(1+\frac{x}{a}\right)\left(1+d\,\frac{x}{a}\right) = c_p\sigma_x \qquad (16)$$

with the solutions

$$x_s = -\frac{a}{2d}(d+1) \pm \frac{a}{2d}\sqrt{(d-1)^2 + \frac{16a^2 c_p d}{3\mu F_z}\sigma_x} \qquad (17)$$

To be able to use the calculation scheme from Section 2, one and only one solution can be inside the contact region. Therefore the sign in front of the square root has to be positive. For d less than -0.5 there are two solutions inside the interval. Physically it means that there are two sliding areas split by one adhesive region. To avoid that, the interval for d is restricted to $[-0.5, 1]$. The total brake force, which is illustrated by the marked area in Figure 3, is described by the integral

$$F_x = \int_{-a}^{x_s} \frac{3\mu F_z}{4a}\left(1 - \left(\frac{x}{a}\right)^2\right)\left(1 + d\,\frac{x}{a}\right) dx + \int_{x_s}^{a} (a-x)\, c_p \sigma_x\, dx \qquad (18)$$

which render the following expression

$$F_x = \frac{\mu F_z}{32d^3}(1-d)^3(3d+1) + \frac{c_p a^2}{4\,d^2}(2d + 5d^2 + 1)\sigma_x + \frac{1}{3}\frac{c_p^2 a^4 \sigma_x^2}{\mu F_z d} - \left(\frac{\mu F_z}{32d^3}(d-1)^2 + \frac{c_p a^2}{6\,d^2}\right)(3d+1)\sigma_x \cdot \sqrt{(d-1)^2 + \frac{16\,d\,c_p \sigma_x a^2}{3\mu F_z}} \qquad (19)$$

The slip limit where the entire contact area slides towards the ground is given by the incline of the pressure curve in $x = a$. Hence,

$$F_x = \mu F_z \quad \text{if} \quad \sigma_x > \frac{3\mu F_z}{2c_p a^2}(1+d) \qquad (20)$$

The result for some different values of d is shown in Figure 7. The complexity of (19) could be reduced by choosing d to 1 or $-1/3$. However, the idea to change the pressure distribution in this way is to get a calibration parameter that can be changed continuously.

3.1.2 Discussion

The resulting expressions for the modified brush model have been compared to a Magic Formula realization of a real tire in this section. The Magic Formula has got a lot of acceptance and it is probably the best model to approximate measurement data to a force-slip function. As mentioned before, it is empirical and not based on the physics and it can be misleading to draw too many conclusions from only comparisons to this reference curve. Besides that, the parabolic pressure distribution gives a good overall fit to the Magic Formula approximation. However, choosing the asymmetric curve with a slightly negative d gives better accuracy specially for lower slip. This is in contradition with the previous discussion about the pressure distribution, but implies that there are other unmodeled factors that affect the shape of the force-slip curve.

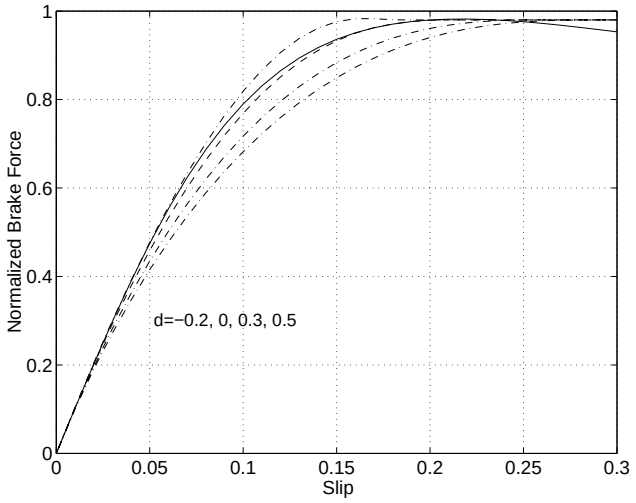

Figure 7: Illustration showing the brake force contra the slip using the pressure distribution given by (15). The solid line denotes a Magic Formula realization from a real tire. The others are derived using different value of d.

3.2 Taylor expansion

Estimation of parameters using schemes as the least squares method are facilitated by use of a simple expression. Therefore, a polynomial approximation for the expression above with parameters depending on d is necessary. Expanding (19) in Taylor series up to order four, for $|d| < 1$, gives

$$F_x = 2\,c_p a^2 \sigma_x + \frac{4}{3}\frac{c_p^2 a^4}{(d-1)\,\mu F_z}\sigma_x^2 - \frac{8}{27}\frac{(3d+1){c_p}^3 a^6}{(d-1)^3\,\mu^2 {F_z}^2}\sigma_x^3 + \frac{16}{27}\frac{(3d+1)\,{c_p}^4 a^8 d}{(d-1)^5\,{F_z}^3 u^3}\sigma_x^4 + \mathrm{O}(\sigma_x^5) \qquad (21)$$

When truncating a series expansion there is always a question about the convergence. In this case it is no restriction to a certain number of terms, but the advantage of the Taylor expansion gets lost if the convergence is slow. If $d = -1/3$ or 0, only 2 respective 3 terms are needed to deliver exact convergence, since d and $(3d+1)$ are parts of the nominator for terms of higher order. For estimation intentions the need of accuracy is discussed in the following section.

3.3 Validation and Simulation

To verify and examine the function of the introduced calibration factor and the accuracy of the Taylor expansion, an optimization was performed. The parameters, $\theta_1 = c_p a^2$ and $\theta_2 = \mu F_z$, included in (21) were choosed to minimize the error between the curve and the real tire data for forces up to 60% of the peak value and with different value on d. The optimization was done for two or three terms. In Figure 8 the results for the obtained parameter values inserted in (19) are shown. It clearly shows the difference when using two or three terms for the optimization. By using a correct calibration factor the effect

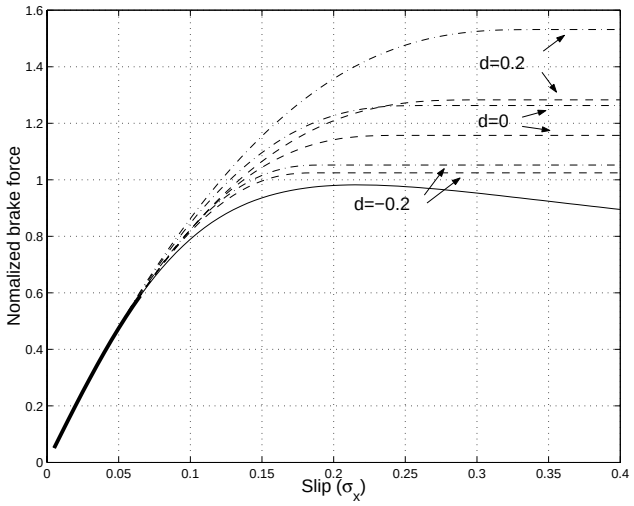

Figure 8: Plot showing optimization of (21) to real tire data with different values of d (Dotted lines: Three terms used, dashed dotted lines: two terms used). The solid line is the Magic Formula representation and the thicker part of it specifies the optimization interval.

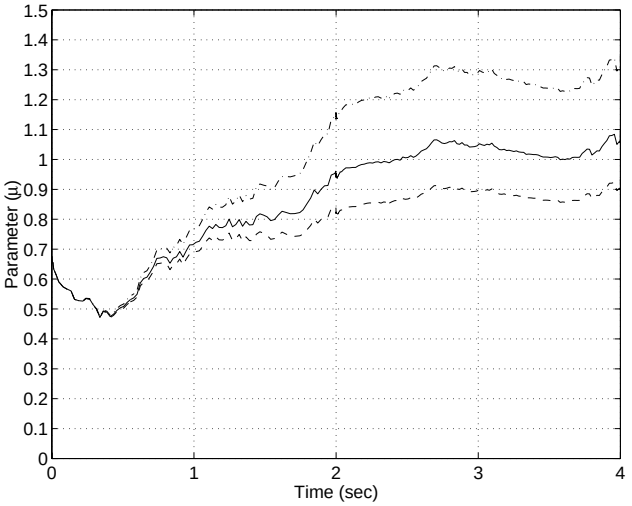

Figure 9: Plot showing the friction estimation using the modified brush-model(21) with two terms and d equal to -0.2 (dashed line), 0 (solid line), and 0.2 (dashed dotted line).

of the truncation can be diminished and an accurate estimation can be achieved for few terms.

Since two terms seems to give accuracy enough for low slip, on-line friction estimation using the recursive least squares method might be performed. This has been verified by simulations, where the input signal, i.e. the brake force, is continuously applied to the tire as a repeated ramp function. The arisen slip is calculated according to the Magic Formula representation previously used in the paper. The maximum value of the input signal is 60% of the peak force value and the corresponding slip is around 4 %. The parameters, $2c_p a^2$ and μF_z is estimated and the resulting μ (assuming constant F_z) is shown in Figure 9. The difference between the estimates is clearly visible, with a of d between -0.2 and 0 giving the estimate best agreement to $\mu = 0.98$.

4 Conclusion

This paper has shown different extensions of how to describe the force-slip curve. A method, with physical interpretation, to introduce an extra parameter to the brush tire model has been discussed. The main result is that the modified brush tire model can be simpler, more flexible, and get a better agreement to the Magic Formula. Further, this new model is better suited for on-line parameter estimation.

References

[1] E. Bakker, H. Pacejka, and L. Lidner. “A new tire model with an application in vehicle dynamics studies.” SAE 890087, 1989.

[2] M. Gäfvert. Topics in Modeling, Control, and Implementations in Automotive Systems. PhD thesis, LTH, 2003.

[3] C.-S. Liu and H. Peng. “Road friction coefficient estimation for vehicle path prediction.” Vehicle system Dynamics, **25**, pp. 413–425, 1996.

[4] H. Pacejka. Modeling of the Pneumatic Tyre and its Impact on Vehicle Dynamic Behavior. Delft, Delft, 1988.

[5] W. R. Pasterkamp and H. B. Pacejka. “The tyre as a sensor to estimate friction.” Vehicle System Dynamics, **27**, 1997.

[6] J. Svendenius. “Wheel model review and friction estimation.” Technical Report TFRT—7607–SE, Department of Automatic Control, LTH, Sweden, 2003.